

# Viscosity, Density and Volatility of Binary Mixtures of Imidazole, 2-Methylimidazole, 2,4,5- Trimethylimidazole and 1,2,4,5- Tetramethylimidazole with Water

*Sigvart Evjen<sup>a</sup>, Ricardo Wanderley<sup>b</sup>, Anne Fiksdahl<sup>a</sup>, Hanna K. Knuutila<sup>b\*</sup>*

a) Department of Chemistry, Norwegian University of Science and Technology, NO-7491

Trondheim, Norway

b) Department of Chemical Engineering, Norwegian University of Science and Technology, NO-7491

Trondheim, Norway

## **Abstract**

Experimental measurements and modelling of the density and viscosity of binary solutions of imidazole, 2-methylimidazole, 2,4,5-trimethylimidazole and 1,2,4,5-tetramethylimidazole with water have been conducted. Parameterization of viscosity data was conducted using a NRTL-model, with AARD of 1% for imidazole, 0.8% for 2-methylimidazole, 3% for 2,4,5-trimethylimidazole and 5% for 1,2,4,5-tetramethylimidazole. The density correlations represent the experimental data for imidazole solutions with AARD of 0.1% for all four imidazoles. Viscosities of aqueous imidazole solutions were found to

increase upon charging solutions with CO<sub>2</sub>. Vapor-liquid equilibrium (P, T, x, y) in the range from 313 to 373 K for the aqueous solutions were performed using ebulliometer. The results show that the tested imidazoles exhibit low vapor pressures in aqueous solutions. Finally, it was found there is an insignificant dependence of water activity on temperature within the range of the present study.

## Introduction

Imidazoles are alkaline *N*-heterocyclic five-membered rings widely present in nature. The primary use of imidazoles are as precursors for more complex structures usable in natural products<sup>1</sup>, such as acylating reagent, stable carbene NHC-ligands<sup>2</sup> and starting materials for ionic liquids<sup>3-4</sup>. Moreover, more recently, simple alkylimidazoles have been discovered to be promising for CO<sub>2</sub> capture applications. We have previously studied the CO<sub>2</sub> absorption capacity of polyalkylated imidazoles and found that high CO<sub>2</sub> absorption capacities are obtainable for these imidazole-based solvents.<sup>5</sup> Imidazoles can also be used to improve CO<sub>2</sub> mass-transfer rates into amine solvents<sup>6</sup> and have been applied to reduce the vapor pressure of volatile organic compounds in aqueous solution.<sup>7</sup> In order to predict and model the behavior of these solvents in separation processes, data about the physical properties of imidazole solutions are required. A few studies covering physical properties of imidazoles and solutions are available. Domanska et al. studied the solubility and densities of a few simple imidazoles in aqueous solution.<sup>8</sup> Shannon et al. found that pure *N*-alkylimidazoles have considerably lower viscosity and density compared to their *N*-alkylimidazolium counterparts.<sup>9</sup> Recently, a thorough investigation of properties of *N*-methylimidazole-H<sub>2</sub>O mixtures was published by Hou et al.<sup>10</sup> These studies cover mono-substituted imidazoles, but as our earlier results have shown that polyalkylated imidazoles are more promising for CO<sub>2</sub> capture related applications, we decided to study the effect of increased substitution on the imidazole-ring.<sup>5</sup> Consequently, data for polyalkylated imidazole is needed in order to model the processes and to evaluate the potential of imidazole-based absorption systems.

In this work, we present the viscosities and densities data for the aqueous blends of four imidazoles, imidazole (Im), 2-methylimidazole (2-Melm), 2,4,5-trimethylimidazole (2,4,5-Melm) and 1,2,4,5-tetramethylimidazole (1,2,4,5-Melm) from 298 to 353 K. The measured viscosities and densities were modelled. Finally, vapor-liquid equilibrium (VLE) measurements of the aqueous solutions provide experimental data on vapor pressure and the relationship between the liquid and gas phase compositions in the range from 313 to 373 K.

## Experimental Section

### Materials

Chemical information is given in Table 1. Aqueous imidazole solutions were prepared on a mass basis (Analytical balance model ME204 with an accuracy of  $2 \cdot 10^{-7}$  kg) using Millipore H<sub>2</sub>O, 18.2  $\Omega$  at 298 K. Partially CO<sub>2</sub> loaded solutions were prepared by bubbling CO<sub>2</sub> into aqueous unloaded imidazole solution. The CO<sub>2</sub> loading was estimated from the weight change and by the wet chemistry methods; the BaCl<sub>2</sub> method<sup>11</sup> and acid-base titration<sup>12</sup>. Acid-base titrations were used to verify imidazole concentrations of unloaded solutions for viscosity and density measurements.

Table 1: Sample Table

Chemical Name	CAS	Source	Initial Mole Fraction Purity	Purification Method	Final Mole Fraction Purity	Analysis Method
Imidazole (Im)	288-32-4	Sigma-Aldrich	$\geq 0.99$			
2-Methylimidazole (2-Melm)	693-98-1	Sigma-Aldrich	0.99			
2,4,5-Trimethylimidazole (2,4,5-Melm)	822-90-2	Synthesis <sup>13</sup>		Distillation	0.98	<sup>1</sup> H NMR
1,2,4,5-Tetramethylimidazole (1,2,4,5-Melm)	1739-83-9	TCI-Europe	0.98			

Monoethanolamine (MEA)	141-43-5	Sigma-Aldrich	$\geq 0.995$
N-Methyldiethanolamine	105-59-9	Sigma-Aldrich	$\geq 0.99$
Carbon dioxide (CO <sub>2</sub> )	124-38-9	AGA	0.99999

### *Viscosity measurements*

Viscosity measurements were performed in a closed system using a viscosity meter (Anton Paar Lovis 2000 ME). The temperature range for the viscosity measurements was 298 to 353 K. Data points were collected by five measurements of the same sample and given as an average. Selected experiments were repeated to calculate repeatability. For controlling the accuracy of the measurements, Millipore H<sub>2</sub>O was run as the first sample for every experimental run and a Millipore H<sub>2</sub>O control sample was run for every five samples tested. Uncertainties in viscosity values are 0.04 mPa·s ( $\eta < 10$  mPa·s), based on calibration data.<sup>14</sup> The repeatability of the experiments was  $\pm 0.1\%$ . Reference liquids used for calibration were 30 wt% MEA<sup>15</sup> and 50 wt% MDEA<sup>16</sup>.

### *Density measurements*

Density measurements were performed using a density meter (Anton Paar DMA 4500). The standard calibration procedure was performed with air and water density measurements at 20 °C. The density of pure water was taken from Spieweck and Bettin.<sup>17</sup> The temperature range for this study was 298 to 353 K. Data points were collected by five measurements of the same sample and given as an average. As in the case of viscosity, selected experiments were repeated to estimate the repeatability and the uncertainty of the measurements was estimated based on density of H<sub>2</sub>O measurements. Millipore H<sub>2</sub>O was run as the first sample for every experimental run and a Millipore H<sub>2</sub>O control sample was run for every five samples tested. Uncertainties and repeatability for density measurements were 2 kg/m<sup>3</sup> and 10<sup>-2</sup> kg/m<sup>3</sup>, respectively.

### *Ebulliometric measurements*

Low pressure vapor-liquid equilibrium (VLE) measurements were performed using a modified Swietoslowski ebulliometer, using modifications by Malanowski.<sup>18</sup> An imidazole solution (105-110 mL) was injected into the apparatus, and the apparatus was purged with N<sub>2</sub> and vacuumed to remove other gases. The apparatus was heated to 313, 333, 353 or 373 K and samples of the liquid and gas phases were taken for at each temperature when VLE had stabilized for 10 minutes. The temperature was measured with a calibrated Pt-100 resistance thermosensors with an uncertainty of  $\pm 0.05$  K. The pressure was measured with a calibrated DPI520 rack mounted pressure controller (Druck Germany), uncertainty of  $\pm 0.3$  kPa. Pressure and temperature were logged online via a Chub-E4 thermometer readout (Hart Scientific, Fluke).

The imidazole concentration in liquid-phase samples was measured by titration with 0.1 M H<sub>2</sub>SO<sub>4</sub> by a Mettler Toledo G20 titrator, and using Lab X3.1 software to determine the equivalence point. Imidazole concentration titration was performed in duplicate and deviation between samples were < 1%. A thorough description of the procedure and uncertainties are given by Kim et al.<sup>19</sup> Validation of the equipment was performed by measuring 30 wt% ethanolamine. Obtained results were within 1% of previously reported values.<sup>19</sup>

Vapor-phase samples were analyzed ion chromatography (IC) with a Thermo Scientific™ Dionex™ ICS-5000 system. Cations were separated using Thermo Scientific Dionex IonPac™ CS19 analytical column (2 mm x 250 mm) with a Thermo Scientific Dionex IonPac™ guard column CG19 (2 mm x 50 mm). In all runs, 20 mM methanesulfonic acid was used as eluent. As suppressor, Thermo Scientific Dionex CSRS 300 2 mm (Cationic Self-Regenerating Suppressor) was used. Chromeleon® 7 was used for in all steps of the analytical method. A complete description of the experimental set-up is described by Fytianos et al.<sup>20</sup> Imidazole standards 5, 10, 20, 40, 60, 80 and 100 ppm were used for interpolation of

sample responses. Samples were diluted once with Millipore water to come within the range of standards. The uncertainty of the IC measurements have previously been investigated by Fytianos et al. using the same equipment and found to be 1%.<sup>20</sup>

### **Modelling**

The modelling performed in this study consists of the parametrization of equations for estimating either viscosity or density. This parametrization proceeds through the minimization of an objective function evaluating the deviation between estimates and results obtained experimentally. For a given set of  $NP$  experimental points  $X$  and estimates  $\hat{X}$ , the objective function was defined as seen in Eq. 1. Furthermore, the average absolute relative deviation (AARD) and the maximum absolute deviation (MAD) are defined as seen in Eqs. 2 and 3 and presented together with the results.

$$F = \sum_{i=1}^{NP} \frac{(X_i - \hat{X}_i)^2}{X_i \hat{X}_i} \quad (1)$$

$$AARD = \frac{100}{NP} \sum_{i=1}^{NP} \frac{|X_i - \hat{X}_i|}{X_i} \quad (2)$$

$$MAD = \max(|X_i - \hat{X}_i|) \quad (3)$$

Both the AARD and the MAD can be used to compare between different alternatives – the lower their values, the more accurate is the model. Another criterion to evaluate the models is the number of adjustable parameters, which ideally should be also low. In this study, no models containing more than six adjustable parameters were considered.

The optimization strategy employed for minimizing the objective function was the Particle Swarm Optimization (PSO) using *lbest* topology, inertia factor  $\omega = 0.7298$  and acceleration coefficients  $\phi_1 = \phi_2 = 1.49618$ , which are the same values employed by Pinto and Svendsen.<sup>21</sup> The exact topology of the PSO as well as the number of particles and of iterations were chosen on a case-by-case basis. A decent run-through on how to implement this algorithm is given by Poli et al.<sup>22</sup> and Ghosh et al.<sup>23</sup>.

### Modelling of viscosity

There are numerous alternatives for modelling the variation of viscosity with temperature and composition in multicomponent mixtures. In general, most of them are written in the form shown in Eq. 4, where NC is the number of components,  $x_i$  is the concentration of each component  $i$  following certain basis (e.g. mass fraction, molar fraction),  $\eta_i^0$  is the viscosity of pure component  $i$  at the desired temperature and  $\Delta\eta$  accounts for the deviation from ideality. Models can therefore differ in how they treat this latter parcel. All equations below are such that the temperature should be given in K, the viscosity in mPa·s and  $x_i$  is the molar fraction of component  $i$ .

$$\ln(\eta(\bar{x}, T)) = \sum_{i=1}^{NC} x_i \ln(\eta_i^0(T)) + \ln(\Delta\eta(\bar{x}, T)) \quad (4)$$

For the purposes of this analysis, the viscosity of pure water  $\eta_w^0$  was calculated using the correlation of Bingham and Jackson shown in Eqs. 5 and 6.<sup>24</sup> For simplicity, the pure imidazoles were considered solids throughout the temperature span. Therefore, imidazole viscosities were set to 1 mPa·s for all temperatures in the following models. From Eq. 4, this means that  $\Delta\eta$  was used for estimating the contribution to the mixture. Although this is a standard course of action and that taken by, for example, Pinto and Svendsen,<sup>21</sup> it increases the stress on the model. To illustrate: at 298 K, this model should combine two substances with roughly the same viscosity (1 mPa·s) to produce a solution with more than 9 mPa·s in the case of 50 wt% 2,4,5-Melm.

$$\phi(T) = 2.1482 \left[ (T - 281.585) + \sqrt{8078.4 + (T - 281.585)^2} \right] - 120 \quad (5)$$

$$\eta_w^0(T) = \frac{100}{\phi(T)} \quad (6)$$

In this study, the models taken into consideration were that of Teng et al.<sup>16</sup> modified by Pinto et al.<sup>25</sup> to take into consideration the effect of temperature, and that of Pinto and Svendsen.<sup>21</sup> These models are briefly discussed below.

Teng et al.<sup>16</sup> describe the viscosity of aqueous amine solutions simply by adding a polynomial term to the viscosity of pure water, which can be seen in Eq. 7. The coefficients of this polynomial may then be parametrized for each temperature. Pinto et al.<sup>25</sup> applied a temperature dependency to these coefficients, seen in Eq. 8, in a way that the same parameters can be employed to estimate viscosity in a range of diverse temperatures and compositions.

$$\ln(\hat{\eta}) = \ln(\eta_w^0) + \sum_{i=1}^{NC} k_i x_i^i \quad (7)$$

$$k_i = a_i + \frac{b_i}{T} \quad (8)$$

The number of parameters for this model naturally will depend on the length of the polynomial expansion, which in turn should be decided upon assessing both accuracy and robustness. Ideally, some statistical treatment should therefore be performed. To compare the different models, a cubic polynomial expansion was chosen for Eq. 7, which implies that six parameters must be estimated.

The model developed by Pinto and Svendsen is shown below in Eqs. 9 – 11.<sup>21</sup> It is inspired by the NRTL activity equations, and for this reason is called the NRTL-DVIS model. It requires four binary parameters per pair of components, and adjustable coefficients  $\alpha_{ij}$  which are typically set to 0.1, 0.2 or 0.3 for all binary interactions at the same time. In this study, no other alternatives for the parameters  $\alpha_{ij}$  were taken into account.

$$\tau_{ij} = a_{ij} + \frac{b_{ij}}{T} \quad ; \quad \tau_{ii} = 0 \quad (9)$$

$$G_{ij} = \exp(-\alpha_{ij}\tau_{ij}) \quad (10)$$

$$\frac{\ln(\Delta\hat{\eta})}{R} = \sum_{i=1}^{NC} x_i \frac{\sum_{j=1}^{NC} \tau_{ji} G_{ji} x_j}{\sum_{k=1}^{NC} G_{ki} x_k} \quad (11)$$

The factor  $R$  in Eq. 11 is picked in a way so that the model can operate with parameters of the same magnitude as those used to model excess Gibbs energy. Pinto and Svendsen optimized theirs to 6.48803 for an ethanolamine-*N*-methyldiethanolamine system, and this value was fixed for  $R$  throughout this work.<sup>21</sup>



### Modelling of density

In this study, it was decided first to estimate the excess molar volume of the imidazole solutions so that their density could be evaluated afterwards, which is the same procedure adopted by Carvalho et al.<sup>26</sup> The excess molar volume of a solution is defined by Eq. 12. In that,  $\rho$  is the density of the mixture while  $\rho_i^0$  is the density of each single component  $i$ .  $M_i$  is the molar mass of component  $i$ . Throughout the following analysis,  $V^E$  will be evaluated in milliliters and all the densities will be given in  $\text{kg/m}^3$ , while molar masses will be inserted in  $\text{m}^3/\text{kmol}$ .

$$V^E(\bar{x}, T) = \frac{\sum_{i=1}^{NC} \frac{x_i}{M_i}}{\rho(\bar{x}, T)} - \sum_{i=1}^{NC} \frac{x_i}{M_i \rho_i^0(T)} \quad (12)$$

With Eq. 12, it is clear that once the excess volume is estimated the solution density should follow swiftly. This is further emphasized in Eq. 13. The models discussed below are for  $V^E$ , whereas the evaluation criteria (AARD, MAD) as well as the objective function in the PSO algorithm are calculated concerning density itself. Eqs. 12 – 13 also make clear that the densities of the pure components are required for this procedure. The pure component densities, assumed constant with temperature for the temperature range, were estimated using the method described by Kotomin and Kozlov<sup>27</sup> using molecular fragment contributions, and their values are shown in Table 2. Meanwhile, the density of water at different temperatures was estimated using the DIPPR105 equation available at the DDBST website and disclosed in Eq. 14.<sup>28</sup>

$$\hat{\rho} = \frac{\sum_{i=1}^{NC} \frac{x_i}{M_i}}{\sum_{i=1}^{NC} \frac{x_i}{M_i \rho_i^0} + \hat{V}^E} \quad (13)$$

$$\rho_w^0 = \frac{0.14395}{0.0112^{1 + \left(1 - \frac{T}{649.727}\right)^{0.05107}}} \quad (14)$$

Table 2: Densities for the pure imidazoles.

	Estimated density (kg/m <sup>3</sup> ) x10 <sup>3</sup>
Im	1.23
2-Melm	1.18
2,4,5-Melm	1.13
1,2,4,5-Melm	1.09

In this study, two models were evaluated for the density calculation. The first was the well-known Redlich-Kister equation as described by de Oliveira and Reis<sup>29</sup> and by Carvalho et al.<sup>26</sup> with a fitting modification to turn its parameters able to operate inside a span of various temperatures. The second was a variation of the NRTL-DVIS viscosity model, designed to estimate  $V^E$  instead.

This Redlich-Kister (R-K) model is presented in Eqs. 15 – 16 for binary solutions only.

$$\hat{V}^E = x_1 x_2 \sum_{i=0}^{NK} A_i (x_1 - x_2)^i \quad (15)$$

$$A_i = a_i + b_i T \quad (16)$$

The parameter fitting for the R-K model was done assuming the imidazole to be component 1 and water to be component 2. It was also decided to stick to a quadratic polynomial expansion, so that six parameters have to be fitted, much similarly to what was done previously with the polynomial expansion for viscosity estimation.

The NRTL inspired model considered in this study is shown in Eq. 17 and requires the same parameters  $\tau_{ij}$ ,  $G_{ij}$  and  $\alpha_{ij}$  calculated in exactly the same way as shown in Eqs. 9 – 10. The pressure and temperature terms were added for consistency with regards to the NRTL equation itself, but it should be noted that  $p$  was set to unity for this analysis. Furthermore, the same value of  $R$  optimized by Pinto and Svendsen<sup>21</sup> was used in this model.

$$\frac{p\hat{V}^E}{RT} = \sum_{i=1}^{NC} x_i \frac{\sum_{j=1}^N \tau_{ji} G_{ji} x_j}{\sum_{k=1}^N G_{ki} x_k} \quad (17)$$

## Results and Discussion

### Viscosity

The viscosity measurements presented for the imidazole-H<sub>2</sub>O mixtures were carried out in the temperature range of 298-353 K at atmospheric pressure. The viscosities of the binary imidazole-H<sub>2</sub>O mixtures are presented in Table 3 and Table 4 shows the measured viscosities of CO<sub>2</sub> loaded solutions. Figures 1 and 2 show the results of the experimental data fitted with the polynomial expansion and NRTL-DVIS for Im. Polynomial expansion and NRTL-DVIS fittings for remaining imidazoles are given in Supporting Information. Comparison between Tables 5 and 6 show that both the polynomial expansion of Teng et al.<sup>16</sup> and the NRTL-DVIS of Pinto and Svendsen fare well for estimating the viscosity of the imidazole solutions, though the former performs better, AARDs in the range of 0.9-1.5% vs 0.8-5.5%.<sup>21</sup> It should be noted, however, that the NRTL-DVIS could be readily expanded to handle multicomponent aqueous mixtures using the same binary interaction parameters, which is something that the polynomial expansion cannot do.

In terms of simplicity, the cubic expansion demanded more parameters (six), while the NRTL-DVIS employs four parameters plus two adjustable handlers that are actually set to the same value. A quadratic polynomial expansion would be also possible, bringing the number of parameters in such model down to four, but this jeopardizes the accuracy of the estimation to the point that it then fares worse than the NRTL-DVIS model.

Table 3: Experimental Viscosities,  $\eta$ , for binary mixtures of imidazoles Im, 2-Melm, 2,4,5-Melm and 1,2,4,5-Melm (1) + H<sub>2</sub>O (w) at 101.3 kPa.<sup>a</sup>

$x_1$	$w_1$	T [K]						
		298.15	303.15	313.15	323.15	333.15	343.15	353.15
		$\eta$ [mPa·s]						
		Im						
0.0286	10 wt%	1.058	0.944	0.771	0.647	0.555	0.486	0.433
0.0621	20 wt%	1.242	1.103	0.892	0.742	0.632	0.549	0.486
0.102	30 wt%	1.470	1.301	1.043	0.862	0.728	0.628	0.551
0.150	40 wt%	1.737	1.541	1.261	1.034	0.865	0.739	0.644
0.209	50 wt%	2.14	1.881	1.543	1.254	1.045	0.863	0.766

2-Melm								
0.0238	10 wt%	1.151	1.020	0.838	0.696	0.591	0.508	0.453
0.0373	15 wt%	1.312	1.160	0.933	0.767	0.647	0.558	0.490
0.0520	20 wt%	1.494	1.315	1.070	0.870	0.713	0.610	0.534
0.0682	25 wt%	1.718	1.498	1.214	0.978	0.792	0.673	0.585
0.0860	30 wt%	1.971	1.707	1.379	1.100	0.886	0.746	0.643
2,4,5-Melm								
0.0179	10 wt%	1.317	1.157	0.944	0.774	0.651	0.552	0.485
0.0393	20 wt%	2.01	1.754	1.384	1.100	0.877	0.736	0.631
0.0655	30 wt%	3.12	2.71	2.08	1.598	1.228	1.010	0.843
0.0983	40 wt%	5.27	4.41	3.24	2.40	1.765	1.407	1.148
0.141	50 wt%	9.35	7.38	4.87	3.44	2.61	2.02	1.618
1,2,4,5-Melm								
0.0159	10 wt%	1.258	1.125	0.899	0.756	0.626	0.541	0.477
0.0350	20 wt%	1.817	1.610	1.244	0.998	0.849	0.696	0.600
0.0585	30 wt%	2.65	2.31	1.733	1.344	1.084	0.894	0.755
0.0882	40 wt%	3.86	3.35	2.53	1.806	1.433	1.154	0.946
0.127	50 wt%	5.77	4.91	3.36	2.44	1.843	1.444	1.166

<sup>a</sup>Standard uncertainties are  $u(T) = 0.01$  K,  $u(x_1) = 0.0002$ ,  $u(\eta) = 0.04$  mPa·s ( $\eta < 10$  mPa·s),  $u(P) = 1.5$  kPa.

For binary imidazole-H<sub>2</sub>O mixtures, the viscosity are in the order Im < 2-Melm < 1,2,4,5-Melm < 2,4,5-Melm. The viscosity of 2,4,5-Melm is greater than 1,2,4,5-Melm due to lack of *N*-H on 1,2,4,5-trimethylimidazole. The overall H-bonding in aqueous mixtures containing *N*-alkylimidazoles is lower than *N*-H imidazoles. However, the viscosity of 1,2,4,5-Melm solutions are still significantly higher than Im- H<sub>2</sub>O or 2-Melm-H<sub>2</sub>O mixtures. On the other hand, Im-H<sub>2</sub>O solutions are less viscous than *N*-methylimidazole-H<sub>2</sub>O solutions.<sup>10</sup> From 298 to 313 K, the viscosity of 30 wt% Im decreases with 29%, and from 313 to 353 K by an additional 47%. For 2,4,5-Melm, the viscosity is reduced by 35% from 25 to 313 K and by 59% from 313 to 353 K.

Table 4: Viscosities of aqueous CO<sub>2</sub> loaded solutions of 30 wt% imidazoles Im, 2-Melm, 2,4,5-Melm and 1,2,4,5-Melm at 298.15 and 313.15 K at 101.3 kPa.<sup>b</sup>

Compound	Loading <sup>a</sup>	T [K]	
		298.15	313.15
		$\eta$ [mPa·s]	
Im	0.19	2.05	1.35
2-Melm	0.40	2.84	1.92

2,4,5-Melm	0.40	- <sup>c</sup>	2.97
1,2,4,5-Melm	0.40	3.85	2.47

<sup>a</sup>Loading is presented as  $\alpha = \text{mol CO}_2/\text{mol imidazole}$ . <sup>b</sup>Standard uncertainties are  $u(T) = 0.01 \text{ K}$ ,  $u(w_1) = 0.2 \text{ wt\%}$ ,  $u(\alpha) = 0.01 \text{ mol CO}_2/\text{mol imidazole}$ ,  $u(P) = 1.5 \text{ kPa}$ . Expanded uncertainty:  $u(\eta) = 0.029 \text{ mPa}\cdot\text{s}$ .

<sup>c</sup>Not measured due to precipitation.

At 313 K, typical minimum temperature conditions in a CO<sub>2</sub> capture plant, the viscosities of all solutions were below 5 mPa·s, as shown in Table 4. Loading 30 wt% imidazole solution with 0.2 mol CO<sub>2</sub>/mol imidazole gave 40% (2.05 mPa·s) and 31% (1.36 mPa·s) higher viscosities at 298 and 313 K, respectively, compared with unloaded imidazole. Solutions containing 30 wt% 2-Melm (1.92 mPa·s), 2,4,5-Melm (2.97 mPa·s) and 1,2,4,5-Melm (2.47 mPa·s) and loaded with 0.4 mol CO<sub>2</sub>/mol imidazole had 40% higher viscosity than unloaded solutions. Consequently, loaded solutions still maintain viscosities well below 5 mPa·s. Viscosities of 2.0-2.2 mPa·s are observed for 30 wt% ethanolamine loaded with 0.4 mol CO<sub>2</sub>/mol amine.<sup>30-31</sup> Diethylethanolamine (30 wt%) and dimethylethanolamine (30 wt%) solutions loaded with 0.4 mol CO<sub>2</sub>/mol amine have viscosities of 2.3-2.5 mPa·s.<sup>32</sup> Thus, viscosities of loaded imidazole are in the same range as aqueous amine solutions.

Table 5: Results of the parameter estimation for viscosity using cubic polynomial expansion.

	Im	2-Melm	2,4,5-Melm	1,2,4,5-Melm
$a_1$	7.348	3.761	-18.94	-12.86
$a_2$	-74.58	-163.4	-55.60	-118.6
$a_3$	198.8	410.2	239.7	439.9
$b_1$	-396.1	2404	12540	10860
$b_2$	17710	32500	-2085	5691
$b_3$	-49950	-34880	-40070	-61890
AARD (%)	0.984	0.875	1.517	1.301
MAD (mPa·s)	0.028	0.034	0.421	0.138

Table 6: Results of the parameter estimation for viscosity using the NRTL-DVIS model.

	Im	2-Melm	2,4,5-Melm	1,2,4,5-Melm
$a_{12}$	27.03	42.91	117.4	87.94

$a_{21}$	14.23	17.23	-5.396	75.06
$b_{12}$	-5429	-9867	-30930	-18980
$b_{21}$	3620	7831	2605	707.1
$\alpha_{12}$	0.3	0.2	0.3	0.1
$\alpha_{21}$	0.3	0.2	0.3	0.1
AARD (%)	1.000	0.750	2.884	5.478
MAD (mPa.s)	0.073	0.047	0.214	0.482

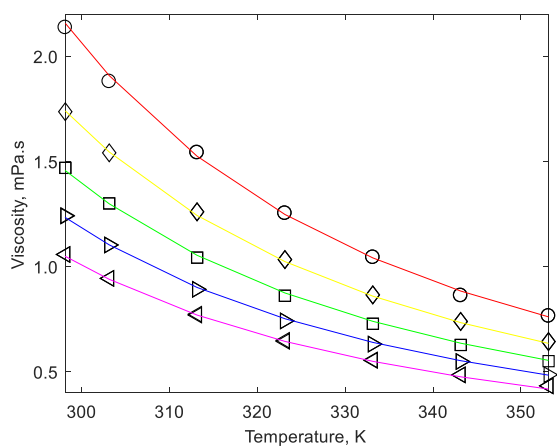


Figure 1: Data and estimation results of the cubic polynomial expansion for Im. Red and O (50 wt%), yellow and  $\diamond$  (40 wt%), green and  $\square$  (30 wt%), blue and  $\triangleright$  (20 wt%), magenta and  $\triangleleft$  (10 wt%).

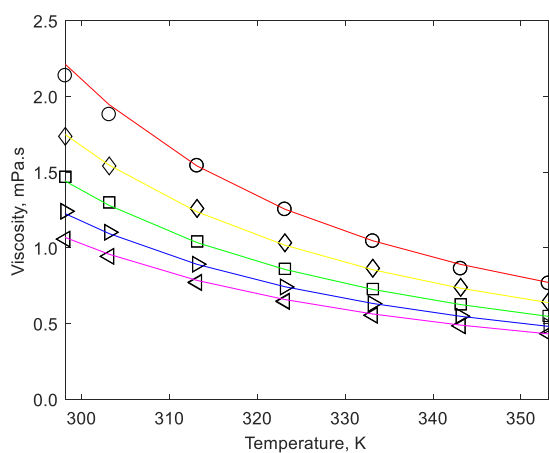


Figure 2: Data and estimation results of the NRTL-DVIS model for Im. Red and O (50 wt%), yellow and  $\diamond$  (40 wt%), green and  $\square$  (30 wt%), blue and  $\triangleright$  (20 wt%), magenta and  $\triangleleft$  (10 wt%).

## Density

The density measurements presented for the imidazole-H<sub>2</sub>O mixtures were carried out in the temperature range of 298-353 K at atmospheric pressure. The densities of the binary imidazole-H<sub>2</sub>O mixtures are presented in Table 7. Density measurements of Im and 2-MeIm at 298 K are compared with results by Domanska et al.<sup>8</sup> in Figure 3, to compare with density data for imidazoles with previously reported values. Domanska et al.<sup>8</sup> ran two series of Im, but got widely different results for the two series of binary solutions as clearly seen in Figure 3 making it difficult to compare the data. However, from the figure it can be seen that our data on 2-MeIm agree well with literature.

The results of parameter fitting are shown in Table 8 and Table 9 for the R-K model and the NRTL-inspired model, It can be seen in Tables 8 and 9 that both R-K (0.08-0.14%) and NRTL (0.08-0.12%) have very decent estimation capacity for the densities of the imidazole solutions. As an improvement from R-K, the NRTL-inspired model has somewhat less parameters once the handlers  $\alpha_{ij}$  are set and has the possibility of being extended to multicomponent solutions. The main challenge associated with the modelling the correlations, are the non-linearity observed for the density of imidazole solutions over the studied range of temperatures and concentrations. Fittings of the NRTL density model for Im-H<sub>2</sub>O systems are presented in Figure 4. Excess volumes and NRTL estimations for 2,4,5-H<sub>2</sub>O solutions are shown in Figure 5. Density fittings for other imidazoles are given in Supporting Information.

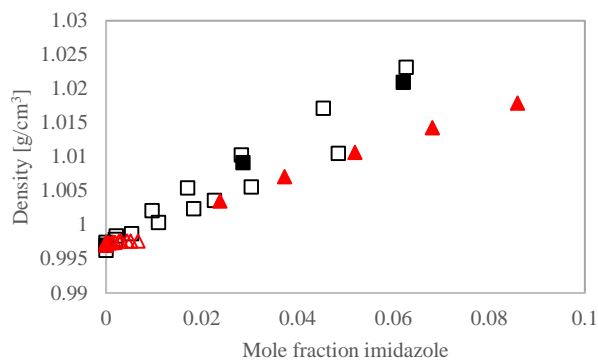


Figure 3: Comparison of imidazole/H<sub>2</sub>O densities at 298 K, Im (□), 2-Melm (△), hollow markers; ref 8, filled markers; this study.

Table 7: Experimental Densities,  $\rho$ , for binary mixtures of imidazoles Im, 2-Melm, 2,4,5-Melm and 1,2,4,5-Melm (1) + H<sub>2</sub>O (w) at 101.3 kPa.<sup>a</sup>

$x_1$	$w_1$	T [K]						
		298.15	303.15	313.15	323.15	333.15	343.15	353.15
		$\rho$ [kg/m <sup>3</sup> ]						
Im								
0.0286	10 wt%	1009.1	1007.3	1003.0	998.2	992.6		
0.0621	20 wt%	1020.9	1018.7	1013.6	1008.2	1002.2	995.8	989.0
0.102	30 wt%	1032.4	1029.7	1024.1	1018.1	1011.6	1004.8	997.6
0.150	40 wt%	1043.4	1040.6	1035.5	1028.9	1022.0	1014.7	1007.2
0.209	50 wt%	1054.1	1051.0	1045.6	1038.8	1031.5	1023.0	1015.2
2-Melm								
0.0238	10 wt%	1003.5	1001.8	998.1	993.4	988.1	981.8	
0.0373	15 wt%	1007.1	1005.2	1000.7	995.7	990.2		
0.0520	20 wt%	1010.7	1008.6	1004.6	999.1	992.7	986.3	979.6
0.0682	25 wt%	1014.3	1011.9	1007.2	1002.9	995.2	988.6	981.7
0.0860	30 wt%	1017.9	1015.4	1010.8	1004.7	997.7	990.9	983.8
2,4,5-Melm								
0.0179	10 wt%	998.7	997.1	993.9	989.2	984.0	977.6	971.3
0.0393	20 wt%	1002.0	1000.0	996.1	990.8	984.4	978.0	971.2
0.0655	30 wt%	1005.6	1003.1	998.4	992.4	985.4	978.6	971.4
0.0983	40 wt%	1008.6	1005.7	1000.0	993.4	985.9	978.6	971.0
0.141	50 wt%	1011.5	1007.1	1000.2	994.1	985.9	978.3	970.3
1,2,4,5-Melm								
0.0159	10 wt%	997.5	995.8	991.7	987.8	981.8	975.9	969.4
0.0350	20 wt%	999.6	997.4	992.5	987.0	981.8	974.6	967.6
0.0585	30 wt%	1002.1	999.5	993.6	987.3	980.8	973.6	966.0
0.0882	40 wt%	1004.9	1001.7	996.1	987.9	980.7	972.8	964.7



0.127	50 wt%	1007.3	1003.7	996.0	988.1	979.9	971.5	962.7
-------	--------	--------	--------	-------	-------	-------	-------	-------

<sup>a</sup>Standard uncertainties  $u(T) = 0.01$  K,  $u(x_1) = 0.0002$ ,  $u(\rho) = 2$  kg/m<sup>3</sup>,  $u(P) = 1.5$  kPa.

By comparing the relative densities of the binary imidazole-H<sub>2</sub>O blends, it can be concluded that the order of densities for the binary systems with water were 1,2,4,5-Melm < 2,4,5-Melm < 2-Melm < Im. The reduction in density with decreased substitution can be rationalized with more H-bonding in aqueous solution. Imidazoles that more readily form H-bonds are able to pack closer together with the water in solution. This trend is in agreement with results by Hou et al. for *N*-methylimidazole-water mixtures, which have lower density than Im-water mixtures.<sup>10</sup>

As seen in Table 7, the density of 1,2,4,5-Melm-H<sub>2</sub>O mixtures are greater than the density of water at temperatures < 318 K. However, above 318 K, the density of mixed systems are greater than for pure water. The same trend is also observed for 2,4,5-Melm, Table 7, where the density of the mixture becomes lower than that of water at ~348 K.

Additional data was extracted from the density; excess molar volume of solution and apparent molar volume. For all binary imidazole-H<sub>2</sub>O mixtures investigated in this study, the excess molar volume was positive, as shown in Figure 5. Greater excess molar volumes are observed at higher temperature for more concentrated imidazole solutions. The increase in excess molar volume can partially be explained by the assumption that Im densities are constant with temperature. The second contribution to the larger excess volumes are that for 2,4,5-Melm-H<sub>2</sub>O and 1,2,4,5-Melm-H<sub>2</sub>O the greater thermal expansion than water is observed. Hence, the excess molar volume of water also increases with temperature.

The apparent molar volume of the imidazoles in aqueous solution,  $\varphi_v$  (cm<sup>3</sup>/mol), can be calculated according to Eq. 18.

$$\varphi_V = \frac{MW}{\rho} - \frac{1000 \cdot (\rho - \rho_w)}{\rho \cdot \rho_w \cdot m} \quad (18)$$

Where MW is the molecular weight of imidazole,  $\rho$  is the measured density of solution,  $m$  is the molality of imidazole in mol/kg and  $\rho_w$  is the density of water. The molar volumes of the imidazoles obtained from Eq. 18 are presented in Table 10. At higher imidazole concentrations, the assumption that the apparent molar volume of water is constant may fail. Both Enea et al.<sup>33</sup> and Jardine et al.<sup>34</sup> were concerned with the properties of Im at infinite dilution. In Figure 6, the data produced in this research are shown against that of Jardine et al.<sup>34</sup> Good agreement between both data sets can be observed. Enea et al.<sup>33</sup> proposed a linear dependency between molality and apparent volume of Im in aqueous solution at 298 K. Figure 6 includes the apparent molar volumes predicted for Im at 298 K, which fit nicely with the results produced at lower Im concentrations both for this work and for that of Jardine et al.

Table 8: Results of the parameter estimation for density using the R-K model.

	Im	2-Melm	2,4,5-Melm	1,2,4,5-Melm
$a_0$	51.72	2214	658.2	946.5
$a_1$	202.73	5309	1798	2534
$a_2$	170.0	3178	1192	1640
$b_0$	-0.136	-7.165	-2.044	-2.980
$b_1$	-0.652	-17.27	-5.733	-8.095
$b_2$	-0.562	-10.35	-3.824	-5.253
AARD (%)	0.078	0.063	0.092	0.081
MAD (kg/m <sup>3</sup> )	3	1	2	2

Table 9: Results of the parameter estimation for density using the NRTL-inspired model.

	Im	2-Melm	2,4,5-Melm	1,2,4,5-Melm
$a_{12}$	12.11	-4.87	1.666	-6.737
$a_{21}$	38.25	72.09	34.46	31.33
$b_{12}$	4539	13932	7146	10070
$b_{21}$	-2083	-7493	-1732	-666.6
$\alpha_{12}$	0.3	0.2	0.3	0.3

$\alpha_{21}$	0.3	0.2	0.3	0.3
AARD (%)	0.072	0.067	0.112	0.118
MAD (kg/m <sup>3</sup> )	3	3	4	4

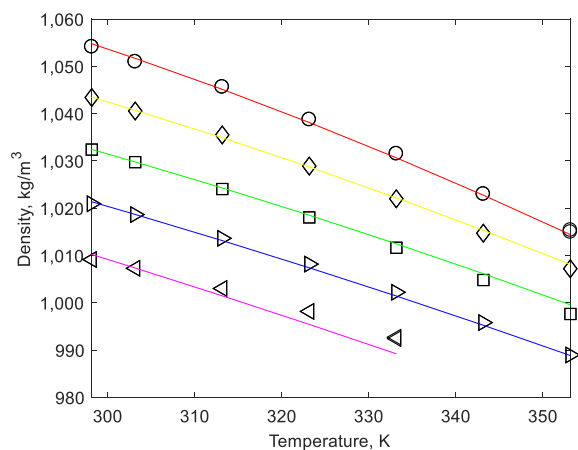


Figure 4: Density and estimation results of the NRTL-inspired model for Im. Red and O (50 wt%), yellow and  $\diamond$  (40 wt%), green and  $\square$  (30 wt%), blue and  $\triangleright$  (20 wt%), magenta and  $\triangleleft$  (10 wt%).

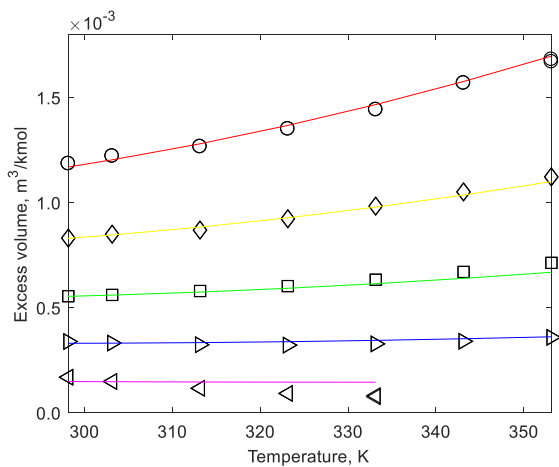


Figure 5: Excess volume and estimation results of the NRTL-inspired model for Im. Red and O (50 wt%), yellow and  $\diamond$  (40 wt%), green and  $\square$  (30 wt%), blue and  $\triangleright$  (20 wt%), magenta and  $\triangleleft$  (10 wt%).

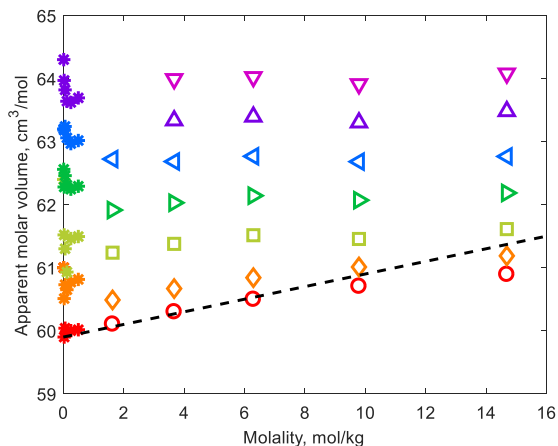


Figure 6: Apparent molar volume for aqueous Im gathered in this work at 101.3 kPa and that of Jardine et al. at 350 kPa, and Enea et al.  $\color{red}\star$ , 298.15 K ref 33;  $\color{orange}\star$ , 308.15 K ref 33;  $\color{green}\star$ , 318.15 K ref 33;  $\color{darkgreen}\star$ , 328.15 K ref 33;  $\color{blue}\star$ , 338.15 K ref 33;  $\color{purple}\star$ , 348.15 K ref 33;  $\color{red}\circ$ , 298.15 K this work;  $\color{orange}\diamond$ , 303.15 K this work;  $\color{green}\square$ , 313.15 K this work;  $\color{green}\triangleright$ , 323.15 K this work;  $\color{blue}\triangleleft$ , 333.15 K this work;  $\color{purple}\triangle$ , 343.15 K this work;  $\color{magenta}\nabla$ , 353.15 K this work; ---, model 298.15 K ref 32.

Table 10: Apparent molar volumes of imidazoles Im, 2-Melm, 2,4,5-Melm and 1,2,4,5-Melm (1) + H<sub>2</sub>O (w) at 101.3 kPa.<sup>a</sup>

$m_1$ [mol/kg solute]	T [K]						
	298.15	303.15	313.15	323.15	333.15	343.15	353.15
$\varphi_v$ [cm <sup>3</sup> /mol]							
Im							
1.63	60.1	60.5	61.2	61.9	62.7		
3.67	60.3	60.7	61.4	62.0	62.7	63.3	64.0
6.29	60.5	60.8	61.5	62.1	62.8	63.4	64.0
9.79	60.7	61.0	61.5	62.1	62.7	63.3	64.0
14.69	60.9	61.2	61.6	62.2	62.8	63.5	64.1
2-Melm							
1.35	77.1	77.4	77.9	78.6	79.4	80.5	
2.15	76.9	77.3	78.1	78.8	79.6		
3.04	76.8	77.2	77.7	78.5	79.5	80.3	81.1
4.06	76.8	77.2	77.7	78.5	79.5	80.3	81.1
5.22	76.7	77.1	77.7	78.5	79.5	80.3	81.1
2,4,5-Melm							
1.01	108.6	109.0	109.2	110.1	111.2	112.8	113.9
2.27	107.7	108.2	108.9	110.0	111.4	112.5	113.7

3.89	107.3	107.9	108.7	109.9	111.2	112.3	113.5
6.05	107.3	107.9	108.9	110.0	111.3	112.4	113.6
9.08	107.3	108.1	109.2	110.1	111.4	112.5	113.7
1,2,4,5-Melm							
0.89	124.0	124.6	125.8	126.0	128.1	129.5	130.9
2.01	123.0	123.6	124.9	126.3	127.2	129.1	130.6
3.45	122.4	123.1	124.6	126.0	127.3	128.8	130.4
5.37	122.1	122.8	123.9	125.7	127.1	128.6	130.1
8.05	122.0	122.7	124.2	125.7	127.1	128.6	130.2

<sup>a</sup>Standard uncertainties are  $u(T) = 0.01$  K,  $u(m_1) = 0.01$  mol/kg solute,  $u(\rho) = 2$  kg/m<sup>3</sup>,  $u(P) = 1.5$  kPa,  $u(\varphi_v) = 0.2$  cm<sup>3</sup>/mol.

### *Ebulliometric measurements*

Tables 11, 12, 13 and 14 present vapor-liquid equilibrium vapor pressures and phase compositions with corresponding water activity coefficient for Im-H<sub>2</sub>O, 2-Melm-H<sub>2</sub>O, 2,4,5-Melm-H<sub>2</sub>O and 1,2,4,5-Melm-H<sub>2</sub>O mixtures, respectively. In this study, equilibrium vapor pressure of pure imidazole solutions were not measured because melting points of the imidazoles were too high for operations in the apparatus (Im: 362 K, 2-Melm 415-416 K, 2,4,5-Melm 406 K, 1,2,4,5-Melm 325-326 K). Imidazoles have substantially higher boiling points than water (Im: 530 K, 2-Melm 540 K, 2,4,5-Melm 543-545 K, 1,2,4,5-Melm 398-401 at 3.8 kPa). In the experiments, the vapor phase primarily contain water as clearly seen in the Tables 11-14. The concentration of imidazoles in the vapor phase is very low at all concentrations. Significantly higher imidazole concentrations in the gas phase are observed for 1,2,4,5-Melm than the *N*-H imidazoles. However, 85% lower vapor pressure was observed for 30 wt% 1,2,4,5-Melm compared to 30 wt% ethanolamine.<sup>19</sup> Thus, negligible loss of the studied imidazoles through evaporation are expected in process conditions. The activity of water can be calculated using the measured variables as described in Van Ness (1995).<sup>35</sup> The data presented in Table 11-14 show that the activity of water in imidazole solutions are slightly higher than for pure water and the water activity seems to be almost independent on the type of imidazole. As the activity increase for water in imidazole solutions is low, adding imidazole can be used to reduce the water vapor pressure. Activity coefficients for the imidazoles

were not calculated in this study, due to lack of experimental data for pure imidazoles. However, as seen from Tables 11-14, the vapor pressure of the imidazoles stay almost constant or is only reduced slightly as the imidazole concentration is reduced. Constant vapor pressure suggests there is a significant increase in the activity coefficient of imidazoles at lower concentrations. This result is in accordance with observations by Domanska et al.<sup>8</sup>

Table 11: VLE Data, mole fractions of the gas and liquid phases ( $x_1$  and  $y_1$ ) and water activity coefficients,  $\alpha_w$ , for Im (1) + H<sub>2</sub>O (w) system depending on composition at 313, 333, 353 and 373 K.<sup>a</sup>

T [K]	P [kPa]	$x_1$	$y_1$	$\alpha_w$
313 K				
313.12	6.29	0.277	0.00015	1.24
313.09	6.49	0.241	0.00014	1.22
313.09	6.69	0.197	0.00014	1.19
313.10	6.78	0.161	0.00013	1.15
313.07	6.89	0.128	0.00010	1.13
333 K				
333.10	16.79	0.279	0.00014	1.20
333.15	17.38	0.239	0.00012	1.17
333.15	17.99	0.195	0.00015	1.15
333.14	18.19	0.161	0.00016	1.11
333.19	18.39	0.131	0.00011	1.08
353 K				
353.13	38.99	0.286	0.00012	1.14
353.17	41.01	0.239	0.00012	1.12
353.17	42.10	0.195	0.00013	1.09
353.17	42.99	0.162	0.00014	1.07
353.17	43.69	0.131	0.00012	1.05
373 K				
373.15	83.27	0.280	0.00019	1.15
373.19	87.51	0.238	0.00016	1.14
373.05	90.10	0.187	0.00015	1.11
373.10	91.78	0.158	0.00015	1.09
373.15	92.98	0.126	0.00012	1.06

<sup>a</sup>Standard uncertainties are  $u(T) = 0.05$  K,  $u(P) = 0.3$  kPa,  $u(x_1) = 0.003$ ,  $u(y_1) = 0.00001$ ,  $u(\alpha_w) = 0.01$ .

Table 12: VLE Data, mole fractions of the gas and liquid phases ( $x_1$  and  $y_1$ ) and water activity coefficients,  $\alpha_w$ , for 2-Melm (1) + H<sub>2</sub>O (w) system depending on composition at 313, 333, 353 and 373 K.<sup>a</sup>

T [K]	P [kPa]	$x_1$	$y_1$	$\alpha_w$
-------	---------	-------	-------	------------

313 K				
313.15	7.19	0.0813	0.00004	1.11
313.10	7.19	0.0682	0.00004	1.10
313.24	7.28	0.0544	0.00003	1.09
313.13	7.28	0.0438	0.00003	1.09
313.33	7.32	0.0379	0.00002	1.07
333 K				
333.21	19.19	0.0816	0.00008	1.07
333.24	19.29	0.0700	0.00007	1.06
333.20	19.39	0.0523	0.00006	1.05
333.09	19.39	0.0426	0.00005	1.04
333.14	19.49	0.0358	0.00005	1.04
353 K				
353.25	45.49	0.0778	0.00013	1.02
353.20	45.58	0.0673	0.00015	1.02
353.14	45.79	0.0527	0.00010	1.01
353.09	45.89	0.0432	0.00013	1.00
353.21	46.00	0.0364	0.00014	0.99
373 K				
373.17	96.68	0.0795	0.00017	1.05
373.09	96.88	0.0680	0.00018	1.04
373.10	97.58	0.0536	0.00016	1.03
373.06	97.87	0.0435	0.00016	1.02
373.12	98.47	0.0369	0.00018	1.02

<sup>a</sup>Standard uncertainties are  $u(T) = 0.05$  K,  $u(P) = 0.3$  kPa,  $u(x_1) = 0.001$ ,  $u(y_1) = 0.00001$ ,  $u(\alpha_w) = 0.01$ .

Table 13: VLE Data, mole fractions of the gas and liquid phases ( $x_1$  and  $y_1$ ) and water activity coefficients,  $\alpha_w$ , for 2,4,5-Melm (1) + H<sub>2</sub>O (w) system depending on composition at 313, 333, 353 and 373 K. <sup>a</sup>

T [K]	P [kPa]	$x_1$	$y_1$	$\alpha_w$
313 K				
313.19	7.29	0.0767	0.00001	1.12
313.12	7.29	0.0588	0.00002	1.10
313.03	7.29	0.0459	0.00001	1.09
313.19	7.39	0.0352	0.00001	1.09
313.07	7.39	0.0183	0.00001	1.08
333 K				
333.16	19.28	0.121	0.00006	1.12
333.06	19.39	0.0915	0.00006	1.10
333.10	19.49	0.0740	0.00005	1.08
333.15	19.59	0.0596	0.00006	1.07
333.21	19.69	0.0446	0.00006	1.05
333.15	19.69	0.0331	0.00004	1.04
333.15	19.79	0.0176	0.00004	1.03
353 K				
353.17	45.79	0.115	0.00009	1.08

353.15	46.09	0.0904	0.00010	1.05
353.18	46.29	0.0741	0.00007	1.04
353.18	46.39	0.0601	0.00008	1.03
353.15	46.48	0.0448	0.00010	1.01
353.20	46.68	0.0335	0.00010	1.00
353.12	46.79	0.0178	0.00008	0.99
373 K				
373.05	97.28	0.117	0.00015	1.10
373.12	98.17	0.0913	0.00016	1.08
373.21	98.77	0.0749	0.00016	1.06
373.19	98.97	0.0603	0.00014	1.05
373.15	99.17	0.0452	0.00013	1.04
373.13	99.37	0.0337	0.00014	1.03
373.09	99.77	0.0180	0.00011	1.02

<sup>a</sup>Standard uncertainties are  $u(T) = 0.05$  K,  $u(P) = 0.3$  kPa,  $u(x_1) = 0.001$ ,  $u(y_1) = 0.00001$ ,  $u(a_w) = 0.01$ .

Table 14: VLE Data, mole fractions of the gas and liquid phases ( $x_1$  and  $y_1$ ) and water activity coefficients,  $\alpha_w$ , for 1,2,4,5-Melm (1) + H<sub>2</sub>O (w) system depending on composition at 313, 333, 353 and 373 K. <sup>a</sup>

T [K]	P [kPa]	$x_1$	$y_1$	$\alpha_w$
313 K				
312.98	6.99	0.131	0.00014	1.16
313.08	7.19	0.0972	0.00014	1.14
313.14	7.19	0.0794	0.00012	1.11
313.15	7.28	0.0695	0.00014	1.11
313.27	7.38	0.0589	0.00013	1.11
313.17	7.39	0.0428	0.00012	1.10
333 K				
333.15	19.18	0.116	0.00032	1.11
333.12	19.38	0.0907	0.00031	1.09
333.14	19.49	0.0787	0.00028	1.09
333.19	19.58	0.0700	0.00023	1.08
333.22	19.69	0.0571	0.00030	1.07
333.13	19.69	0.0420	0.00028	1.06
353 K				
353.10	45.38	0.118	0.00055	1.07
353.08	45.89	0.0914	0.00054	1.05
353.08	46.09	0.0796	0.00053	1.05
353.13	46.29	0.0708	0.00056	1.04
353.14	46.49	0.0574	0.00043	1.03
353.15	46.69	0.0425	0.00044	1.01
373 K				
373.12	97.37	0.111	0.00082	1.10
373.09	98.17	0.0920	0.00079	1.08



373.07	98.48	0.0799	0.00080	1.07
373.12	98.88	0.0713	0.00079	1.06
373.13	99.28	0.0587	0.00071	1.05
373.16	99.78	0.0437	0.00067	1.04

<sup>a</sup>Standard uncertainties are  $u(T) = 0.05$  K,  $u(P) = 0.3$  kPa,  $u(x_1) = 0.001$ ,  $u(y_1) = 0.00002$ ,  $u(a_w) = 0.01$ .

## Conclusion

In this study, density, viscosity and ebulliometric measurements of binary mixtures of water with four different imidazoles, Im, 2-Melm, 2,4,5-Melm and 1,2,4,5-Melm were performed and the experimental viscosity and density data was modelled. The viscosities of all solutions were below 3 mPa·s at temperatures above 313 K. Parameterization of viscosity data was conducted using a NRTL-model, with AARD of 1% for Im, 0.8% for 2-Melm, 3% for 2,4,5-Melm and 5% for 1,2,4,5-Melm. The density correlations represent the experimental data for imidazole solutions with AARD of 0.1% for Im, 2-Melm, 2,4,5-Melm and 1,2,4,5-Melm. VLE measurements containing pressure, temperature, and the composition of both phases ( $P$ ,  $T$ ,  $x$ ,  $y$ ) in the range from 313 to 373 K for aqueous solutions of Im, 2-Melm, 2,4,5-Melm and 1,2,4,5-Melm are given. The results show that the tested imidazoles exhibit low vapor pressures in aqueous solutions. Finally, it was found there is an insignificant dependence of water activity on temperature within the range of the present study.

## Additional Information

Supporting Information Available: Viscosity and density model fittings (docx).

## Corresponding Author

Corresponding author: hanna.knuutila@ntnu.no, telephone: +47 735 94119

## Acknowledgements

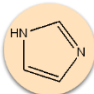
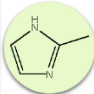
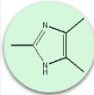
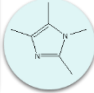
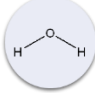
The authors would like to acknowledge the financial support of the Research Council of Norway, through CLIMIT grant 233776. Blanca Yuritz Cervantes Gameros is acknowledge for running MDEA calibration solutions.

## References

1. Zhang, L.; Peng, X.-M.; Damu, G. L. V.; Geng, R.-X.; Zhou, C.-H., Comprehensive Review in Current Developments of Imidazole-Based Medicinal Chemistry. *Med. Res. Rev.* **2014**, *34*, 340-437.
2. Fortman, G. C.; Nolan, S. P., N-Heterocyclic carbene (NHC) ligands and palladium in homogeneous cross-coupling catalysis: a perfect union. *Chem. Soc. Rev.* **2011**, *40*, 5151-5169.
3. Huddleston, J. G.; Visser, A. E.; Reichert, W. M.; Willauer, H. D.; Broker, G. A.; Rogers, R. D., Characterization and comparison of hydrophilic and hydrophobic room temperature ionic liquids incorporating the imidazolium cation. *Green Chem.* **2001**, *3*, 156-164.
4. Lee, S.-g., Functionalized imidazolium salts for task-specific ionic liquids and their applications. *Chem. Commun.* **2006**, 1049-1063.
5. Evjen, S.; Fiksdahl, A.; Pinto, D. D. D.; Knuutila, H. K., New polyalkylated imidazoles tailored for carbon dioxide capture. *Int. J. Greenhouse Gas Control* **2018**, *76*, 167-174.
6. Du, Y.; Yuan, Y.; Rochelle, G. T., Capacity and absorption rate of tertiary and hindered amines blended with piperazine for CO<sub>2</sub> capture. *Chem. Eng. Sci.* **2016**, *155*, 397-404.
7. Puxty, G.; Conway, W.; Botma, H.; Feron, P.; Maher, D.; Wardhaugh, L., A New CO<sub>2</sub> Absorbent Developed from Addressing Benzylamine Vapour Pressure Using Co-solvents. *Energy Procedia* **2017**, *114*, 1956-1965.
8. Domanska, U.; Kozłowska, M. K.; Rogalski, M., Solubilities, partition coefficients, density, and surface tension for imidazoles plus octan-1-ol or plus water or plus n-decane. *J. Chem. Eng. Data* **2002**, *47*, 456-466.
9. Shannon, M. S.; Bara, J. E., Properties of Alkylimidazoles as Solvents for CO<sub>2</sub> Capture and Comparisons to Imidazolium-Based Ionic Liquids. *Ind. Eng. Chem. Res.* **2011**, *50*, 8665-8677.
10. Hou, H.; Jiao, B.; Li, Q.; Lin, X.; Liu, M.; Shi, H.; Wang, L.; Liu, S., Physicochemical properties, NMR, Ab initio calculations and the molecular interactions in a binary mixture of N-methylimidazole and water. *J. Mol. Liq.* **2018**, *257*, 100-111.
11. Ma'mun, S.; Jakobsen, J. P.; Svendsen, H. F.; Juliusen, O., Experimental and modeling study of the solubility of carbon dioxide in aqueous 30 mass % 2-((2-aminoethyl)amino)ethanol solution. *Ind. Eng. Chem. Res.* **2006**, *45*, 2505-2512.
12. Hartono, A.; Saleem, F.; Arshad, M. W.; Usman, M.; Svendsen, H. F., Binary and ternary VLE of the 2-(diethylamino)-ethanol (DEEA)/3-(methylamino)-propylamine (MAPA)/water system. *Chem. Eng. Sci.* **2013**, *101*, 401-411.
13. Evjen, S.; Fiksdahl, A., Syntheses of polyalkylated imidazoles. *Synth. Commun.* **2017**, *47*, 1392-1399.
14. Huber, M. L.; Perkins, R. A.; Laesecke, A.; Friend, D. G.; Sengers, J. V.; Assael, M. J.; Metaxa, I. N.; Vogel, E.; Mareš, R.; Miyagawa, K., New International Formulation for the Viscosity of H<sub>2</sub>O. *J. Phys. Chem. Ref. Data* **2009**, *38*, 101-125.
15. Hartono, A.; Mba, E. O.; Svendsen, H. F., Physical Properties of Partially CO<sub>2</sub> Loaded Aqueous Monoethanolamine (MEA). *J. Chem. Eng. Data* **2014**, *59*, 1808-1816.
16. Teng, T. T.; Maham, Y.; Hepler, L. G.; Mather, A. E., Viscosity of Aqueous Solutions of N-Methyldiethanolamine and of Diethanolamine. *J. Chem. Eng. Data* **1994**, *39*, 290-293.
17. Spieweck, F.; Bettin, H., Solid and Liquid Density Determination. *Tech. Mess.* **1992**, *59*, 237-244.
18. Rogalski, M.; Malanowski, S., Ebulliometers Modified for the Accurate Determination of Vapor-Liquid-Equilibrium. *Fluid Phase Equilib.* **1980**, *5*, 97-112.

19. Kim, I.; Svendsen, H. F.; Børresen, E., Ebulliometric Determination of Vapor–Liquid Equilibria for Pure Water, Monoethanolamine, N-Methyldiethanolamine, 3-(Methylamino)-propylamine, and Their Binary and Ternary Solutions. *J. Chem. Eng. Data* **2008**, *53*, 2521-2531.
20. Fytianos, G.; Callot, R.; Svendsen, H. F.; Knuutila, H. K., Quantitative determination of amines used in post-combustion CO<sub>2</sub> capture process by ion chromatography. *Int. J. Greenhouse Gas Control* **2015**, *42*, 372-378.
21. Pinto, D. D. D.; Svendsen, H. F., An excess Gibbs free energy based model to calculate viscosity of multicomponent liquid mixtures. *Int. J. of Greenhouse Gas Control* **2015**, *42*, 494-501.
22. Poli, R.; Kennedy, J.; Blackwell, T., Particle swarm optimization. *Swarm Intelligence* **2007**, *1*, 33-57.
23. Ghosh, S.; Das, S.; Kundu, D.; Suresh, K.; Abraham, A., Inter-particle communication and search-dynamics of lbest particle swarm optimizers: An analysis. *Inf. Sci.* **2012**, *182*, 156-168.
24. Bingham, E. C.; Jackson, R. F., Standard substances for the calibration of viscometers. *J. Franklin Inst.* **1917**, *183*, 229-230.
25. Pinto, D. D. D.; Monteiro, J. G. M. S.; Johnsen, B.; Svendsen, H. F.; Knuutila, H., Density measurements and modelling of loaded and unloaded aqueous solutions of MDEA (N-methyldiethanolamine), DMEA (N,N-dimethylethanolamine), DEEA (diethylethanolamine) and MAPA (N-methyl-1,3-diaminopropane). *Int. J. Greenhouse Gas Control* **2014**, *25*, 173-185.
26. Carvalho, P. J.; Regueira, T.; Santos, L. M. N. B. F.; Fernandez, J.; Coutinho, J. A. P., Effect of Water on the Viscosities and Densities of 1-Butyl-3-methylimidazolium Dicyanamide and 1-Butyl-3-methylimidazolium Tricyanomethane at Atmospheric Pressure. *J. Chem. Eng. Data* **2010**, *55*, 645-652.
27. Kotomin, A. A.; Kozlov, A. S., Calculation of densities of organic compounds from contributions of molecular fragments. *Russ. J. Appl. Chem.* **2006**, *79*, 957-966.
28. Dortmund Data Bank, DDBST GmbH. <http://www.ddbst.com/> (accessed 4 March).
29. de Oliveira, J. D. G.; Reis, J. C. R., The two faces of the Redlich–Kister equation and the limiting partial molar volume of water in 1-aminopropan-2-ol. *Thermochim. Acta* **2008**, *468*, 119-123.
30. Amundsen, T. G.; Øi, L. E.; Eimer, D. A., Density and Viscosity of Monoethanolamine + Water + Carbon Dioxide from (25 to 80) °C. *J. Chem. Eng. Data* **2009**, *54*, 3096-3100.
31. Zhang, J.; Fennell, P. S.; Trusler, J. P. M., Density and Viscosity of Partially Carbonated Aqueous Tertiary Alkanolamine Solutions at Temperatures between (298.15 and 353.15) K. *J. Chem. Eng. Data* **2015**, *60*, 2392-2399.
32. Patzschke, C. F.; Zhang, J.; Fennell, P. S.; Trusler, J. P. M., Density and Viscosity of Partially Carbonated Aqueous Solutions Containing a Tertiary Alkanolamine and Piperazine at Temperatures between 298.15 and 353.15 K. *J. Chem. Eng. Data* **2017**, *62*, 2075-2083.
33. Enea, O.; Jolicoeur, C.; Hepler, L. G., Apparent Molar Heat-Capacities and Volumes of Unsaturated Heterocyclic Solutes in Aqueous-Solution at 25-Degrees-C. *Can. J. Chem.* **1980**, *58*, 704-707.
34. Jardine, J. J.; Patterson, B. A.; Origlia-Luster, M. L.; Woolley, E. M., Thermodynamics for proton dissociation from aqueous imidazolium ion at temperatures from 278.15 K to 393.15 K and at the pressure 0.35 MPa: apparent molar volumes and apparent molar heat capacities of the protonated and neutral imidazole. *J. Chem. Thermodyn.* **2002**, *34*, 895-913.
35. Van Ness, H. C., Thermodynamics in the Treatment of Vapor-Liquid-Equilibrium (Vle) Data. *Pure Appl. Chem.* **1995**, *67*, 859-872.

## For Table of Contents Only

Viscosity Density Volatility		imidazole
		2-Methylimidazole
		2,4,5-Trimethylimidazole
		1,2,4,5-Tetramethylimidazole
		Water